Supplementary Material
Gold, Carbon and Aluminum Low-reflectivity Compact Discs as Microassaying Platforms

Eva M. Brun, Rosa Puchades, and Ángel Maquieira*

Centro de Reconocimiento Molecular y Desarrollo Tecnológico,
Departamento de Química, Universidad Politécnica de Valencia,
Camino de Vera s/n, 46022 Valencia, Spain

A

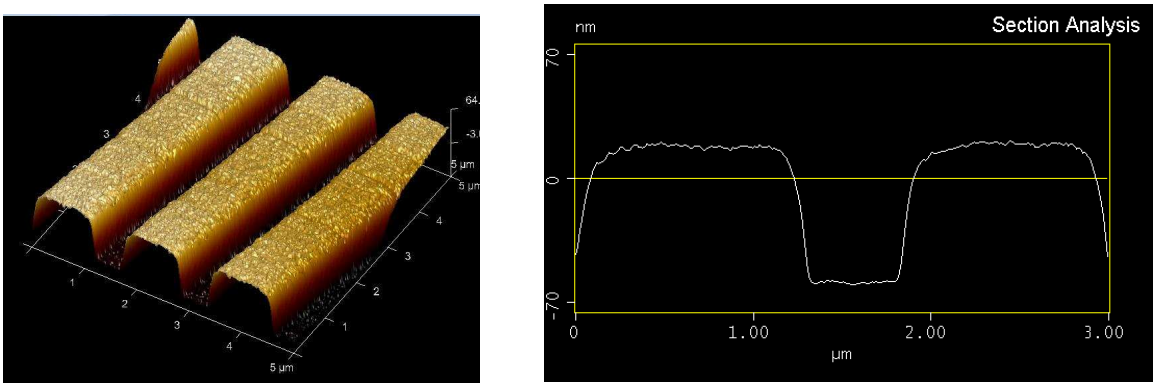

B

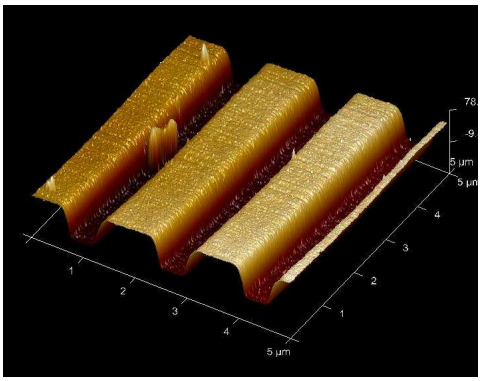

C

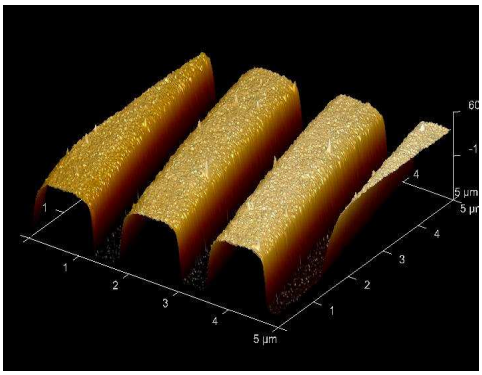

Figure S1. AFM image of a (5 µm × 5 µm) exposed layer for (A) gold, with the corresponding cross-sectional profile, (B) carbon, (C) aluminum L-CD.

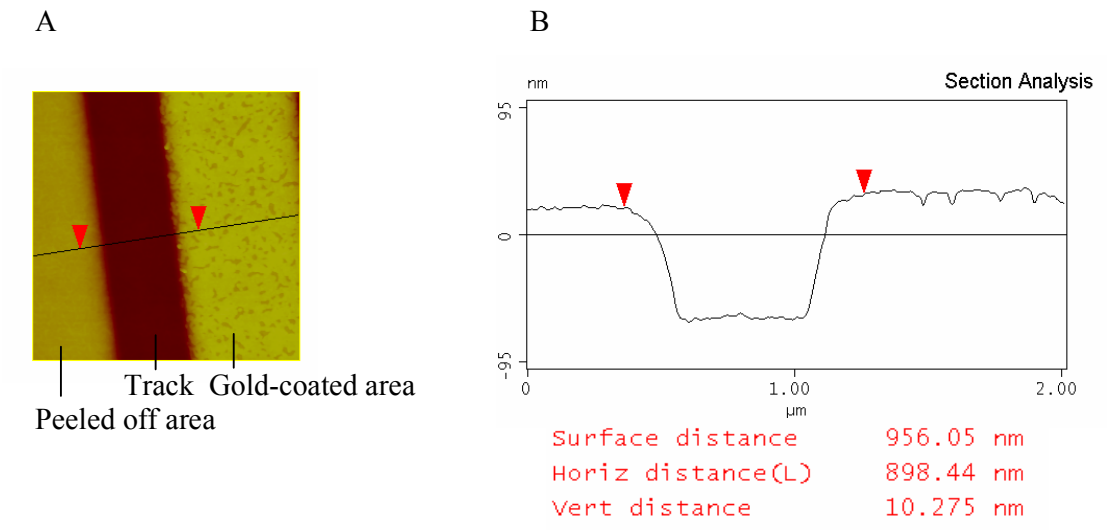

Figure S2. Gold thickness AFM measurement. (A) AFM image of a peeled off gold L-CD (2 x 2 μm^2). The gold has been removed on the left of the CD track, but is present on the right. (B) Cross-sectional profile of (A). Vertical distance between track sides is around 10 nm.

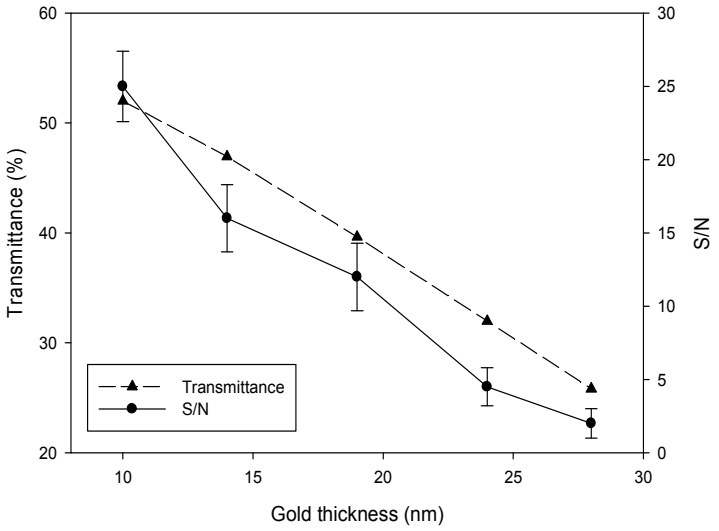

Figure S3. Transmittance and S/N values (mean value ± standard deviation of 91 replicates) related to gold film thickness.

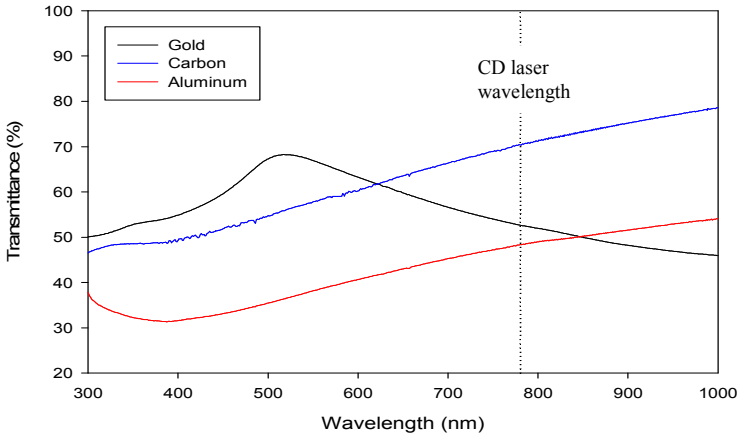

Figure S4. UV-VIS spectra of the developed gold, carbon and aluminum L-CDs. A CD polycarbonate base was used as blank.

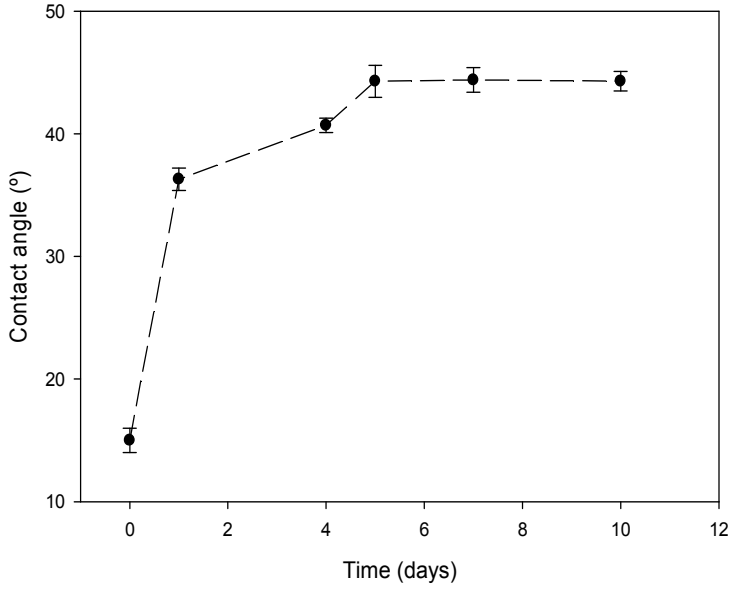

Figure S5. Variation of water contact angle of a carbon-coated CD surface as a function of storage time.

A

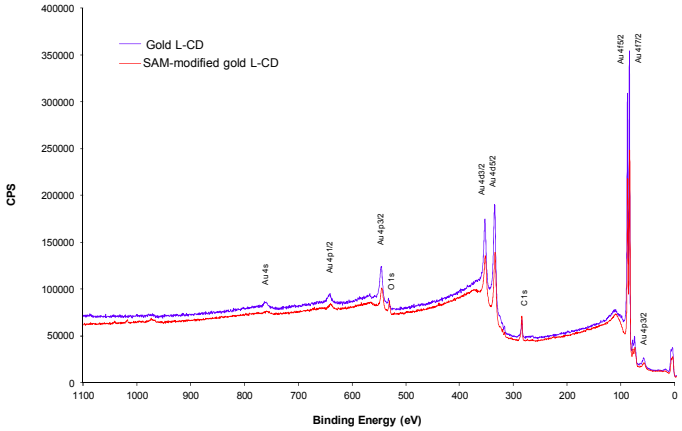

B

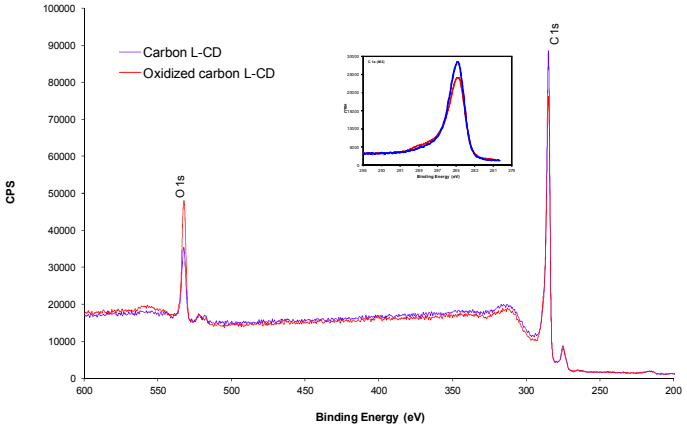

C

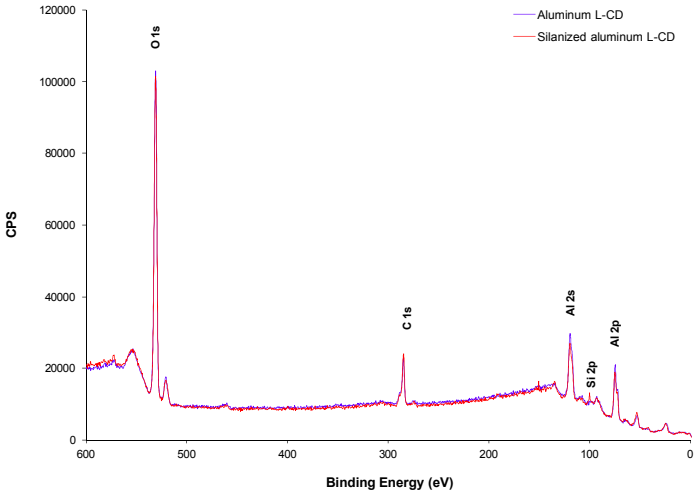

Figure S6. Superposed overview XPS spectra of L-CDs: (A) original and SAM-modified gold, (B) carbon and oxidized carbon, (C) aluminum and silanized aluminum. (B) inset: Detailed C 1s XPS spectra from carbon (blue) and an oxidized carbon L-CD (red).

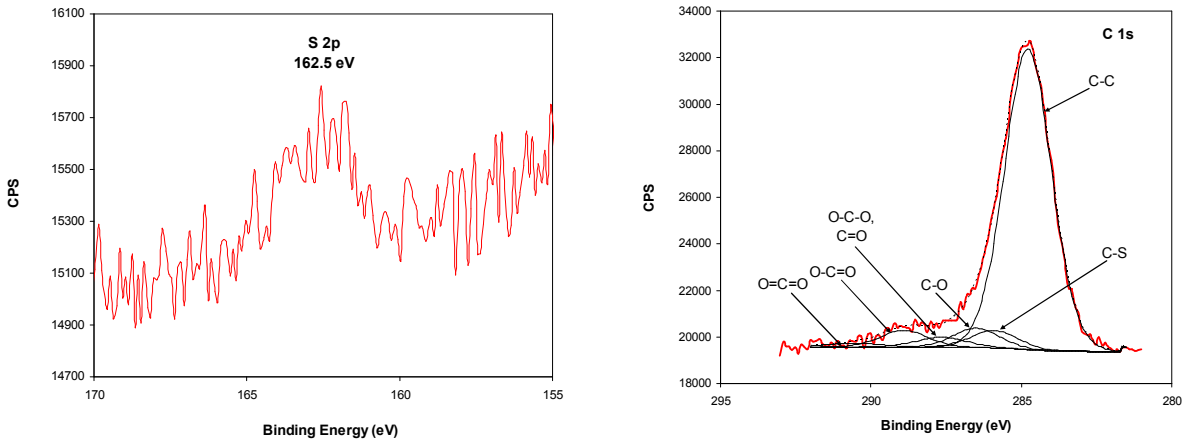

Figure S7. XPS spectra of the S 2p and C 1s core levels from an 11-MUA SAM-modified gold L-CD.

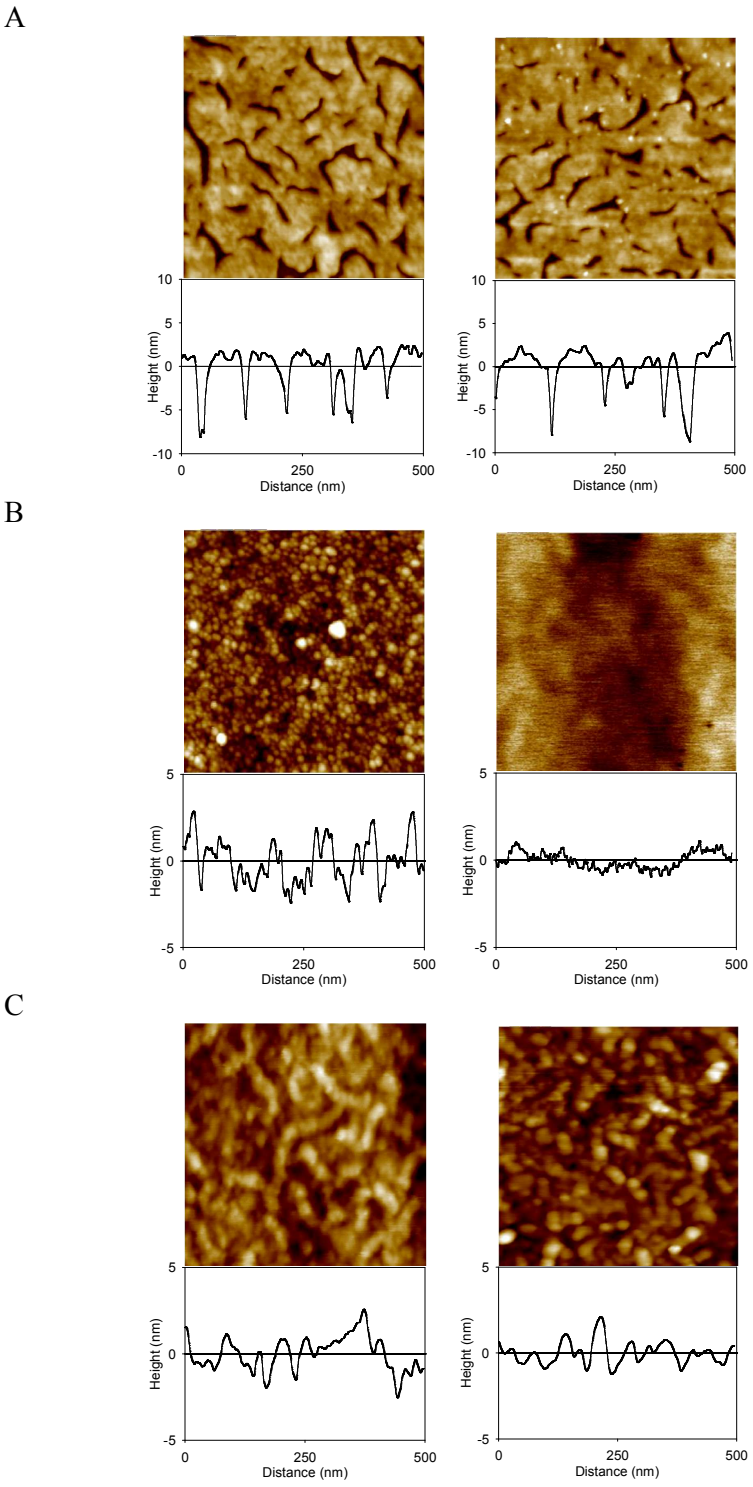

Figure S8. AFM topographic images (500 × 500 nm^2) and section profiles of (A) gold L-CD top surface (left) and 11-MUA SAM-modified L-CD (right), (B) carbon L-CD surface (left) and oxidized carbon L-CD (right), and (C) aluminum L-CD surface (left) and silanized aluminum L-CD (right).

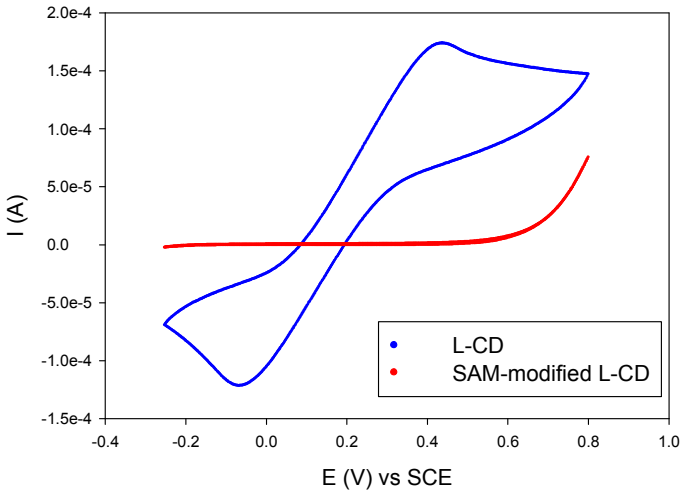

Figure S9. Cyclic voltammograms (scan rate 10 mV/s) on bare and SAM-modified gold L-CDs in aqueous electrolytes containing 5 mM KNO_3 and 5 mM $K_4Fe(CN)_6$.

A

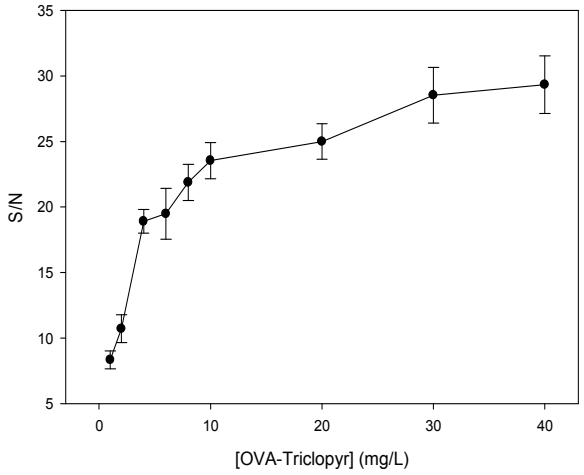

B

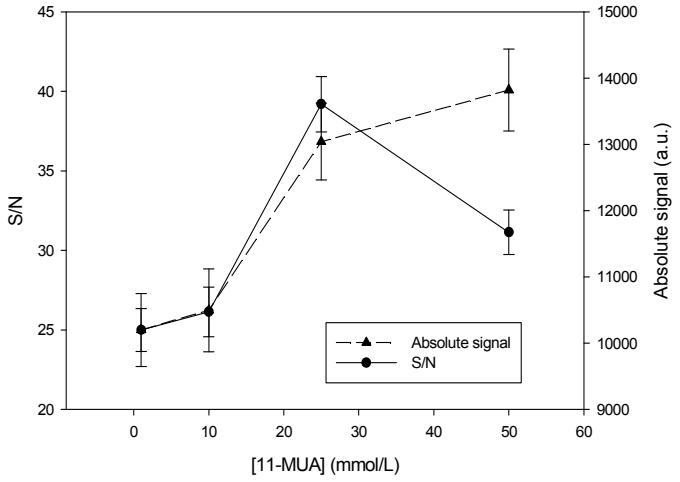

Figure S10. S/N values (mean value ± standard deviation of 48 replicates) obtained from CD drive read-outs after the immunoassay depending on the concentration of (A) protein-hapten conjugate and (B) 11-MUA.

A) Covalent linking

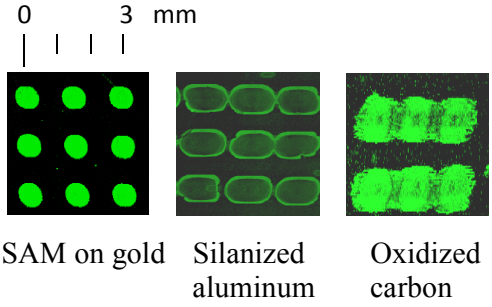

B) Passive adsorption

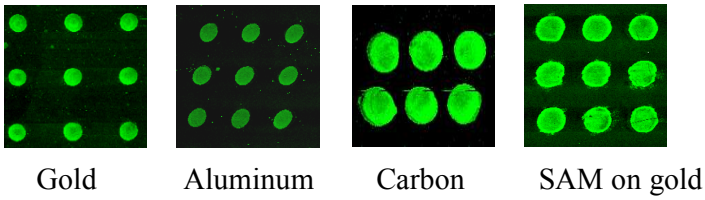

Figure S11. Images obtained for the different surfaces after CD reading, corresponding to a chlorpyrifos concentration of 0 µg/L.

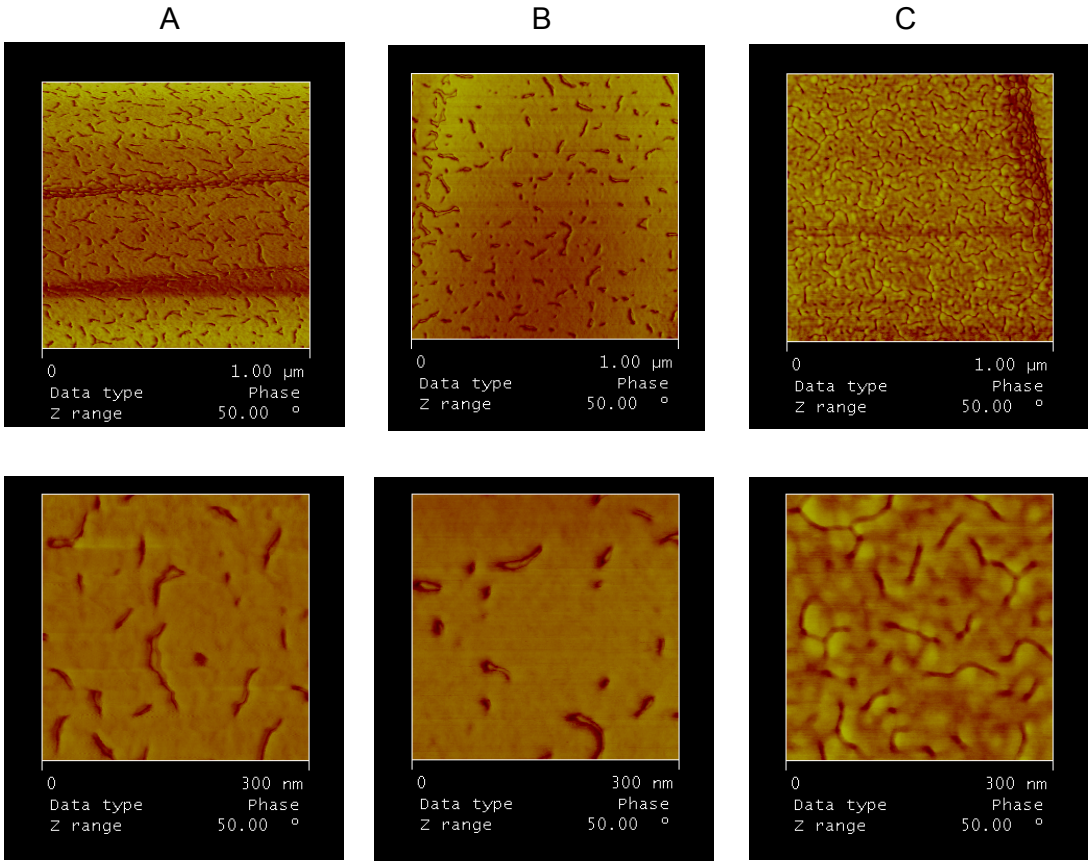

Figure S12. 1×1 µm^2 and 300×300 nm^2 AFM topographic images of (A) gold L-CD top surface, (B) 11-MUA SAM-modified L-CD, (C) Conjugate OVA-triclopyr adsorbed onto a SAM-modified L-CD.

Table S1. Layer thickness, reflectivity and transmittance of L-CDs.

Material surface	*Layer thickness (nm)*	*% Reflectivity (780 nm)*	*% Transmittance (780 nm)*
Gold	10.2 ± 0.5	32	52
Carbon	35.1 ± 4.6	28	72
Aluminum	16.7 ± 0.6	25	48

Table S2. Wetting characteristics of the studied surfaces.

CD top layer	*Contact angle (°)*	*Spot size (μm)**
Gold	79.2 ± 1.0	561 ± 12
SAM-modified gold	47.5 ± 0.3	741 ± 19
Carbon	44.3 ± 1.3	923 ± 12
Oxidized carbon	15.6 ± 0.4	1168 ± 45
Aluminum	56.3 ± 0.8	621 ± 18
Silanized aluminum	28.5± 0.3	1023± 46

*Printed volume: 20 nL.

Table S3. Elemental composition determined by XPS of (A) gold and SAM-modified gold L-CD, (B) carbon and oxidized carbon L-CD, (C) aluminum and silanized aluminum L-CD.

(A)

Element	Gold L-CD	SAM-modified gold L-CD
O 1s (%)	5.7	10.0
C 1s (%)	40.3	57.0
S 2p (%)	-	2.5
Au 4f (%)	54.0	30.5

(B)

Element	Carbon L-CD	Oxidized carbon L-CD
O 1s (%)	10.0	16.0
C 1s (%)	90.0	84.0

(C)

Element	Aluminum L-CD	Silanized aluminum L-CD
O 1s (%)	44.9	46.8
Al 2p (%)	38.1	32.3
C 1s (%)	17.0	19.4
Si 2p (%)	-	1.5